NANO LETTERS

Letter

pubs.acs.org/NanoLett

Improved Light Harvesting and Improved Efficiency by Insertion of an Optical Spacer (ZnO) in Solution-Processed Small-Molecule Solar Cells

Aung Ko Ko Kyaw,[†,‡] Dong Hwan Wang,[†] David Wynands,[†] Jie Zhang,[‡] Thuc-Quyen Nguyen,[†] Guillermo C. Bazan,[†] and Alan J. Heeger*[,†]

[†]Center for Polymers and Organic Solids, University of California at Santa Barbara, Santa Barbara, California 93106-5090, United States

[‡]Institute of Materials Research and Engineering, Agency for Science Technology and Research (A*STAR), Singapore 11760, Republic of Singapore

Supporting Information

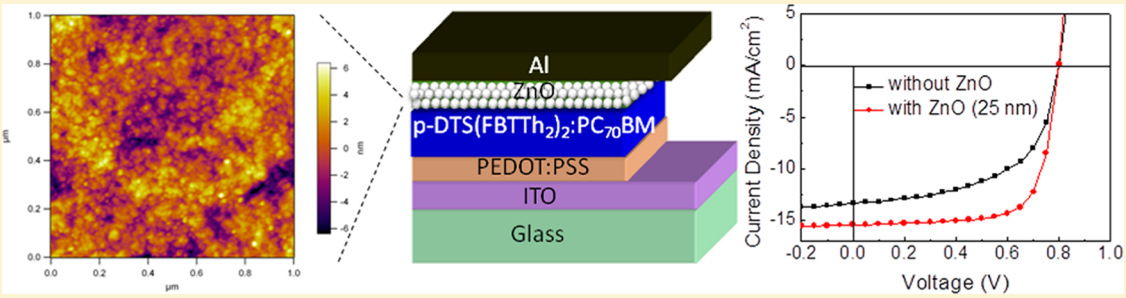

ABSTRACT: We demonstrate that the power conversion efficiency can be significantly improved in solution-processed small-molecule solar cells by tuning the thickness of the active layer and inserting an optical spacer (ZnO) between the active layer and the Al electrode. The enhancement in light absorption in the cell was measured with UV−vis absorption spectroscopy and by measurements of the photoinduced carriers generation rate. The ZnO layer used to improve the light-harvesting increases the charge collection efficiency, serves as a blocking layer for holes, and reduces the recombination rate. The combined optical and electrical improvements raise the power conversion efficiency of solution-processed small-molecule solar cells to 8.9%, that is, comparable to that of polymer counterparts.

KEYWORDS: *Solution-processed small-molecule solar cell, optical spacer, ZnO nanoparticle, recombination*

Recently, organic solar cells (OSC) based on solution-processed small-molecule (SM) donors have attracted attention as a competitive alternative to widely used conjugated polymer-based donors.[1−6] For commercial applications, solution-processed SM donors offer relatively simple synthesis and purification, monodispersity, and well-defined structures without end group contaminants, relatively high charge carrier mobility, and better batch-to-batch reproducibility. A power conversion efficiency (PCE) of more than 8% has been reported with a conventional architecture and 7.88% with an inverted structure using a solution-processed SM donor: 7,7′-(4,4-bis(2-ethylhexyl)-4*H*-silolo[3,2-*b*:4,5-b′]dithiophene-2,6-diyl)bis(6-fluoro-4-(5′-hexyl-[2,2′-bithiophen]-5-yl)benzo[*c*]-[1,2,5] thiadiazole) (*p*-DTS(FBTTh$_2$)$_2$).[4,5,7]

Similar to other thin film solar cells, however, the design and optimization of the solution-processed SM solar cell is challenged by the mismatch between optical absorption length and charge transport scale.[8−10] Increasing the thickness of the active layer increases the probability of charge recombination and decreases the carrier drift velocity by reducing the internal electric field. Therefore, structuring the solution-processed SM solar cell so that more light is harvested inside the active layer to increase the optical absorption within a film of limited thickness is very important.

Traditionally, surface texturing is used to increase cell absorption by scattering of light and to reduce reflection in conventional thick-silicon solar cells.[8,11] However, texturing is practically challenging for organic solar cells because of difficulties in the formation of nanometer-scale-thick conformal films on topographical surfaces.[12] Other light trapping strategies are being explored to improve the light-harvesting efficiency in optically thin OSC including periodic nanostructures, the use of microcavities, and photonic crystals.[13−17] Nevertheless, there are concerns about processing bottlenecks and drawbacks in making periodic patterns, especially in the active layer.

Received: May 13, 2013
Revised: June 19, 2013

   dx.doi.org/10.1021/nl401758g | *Nano Lett.* XXXX, XXX, XXX−XXX

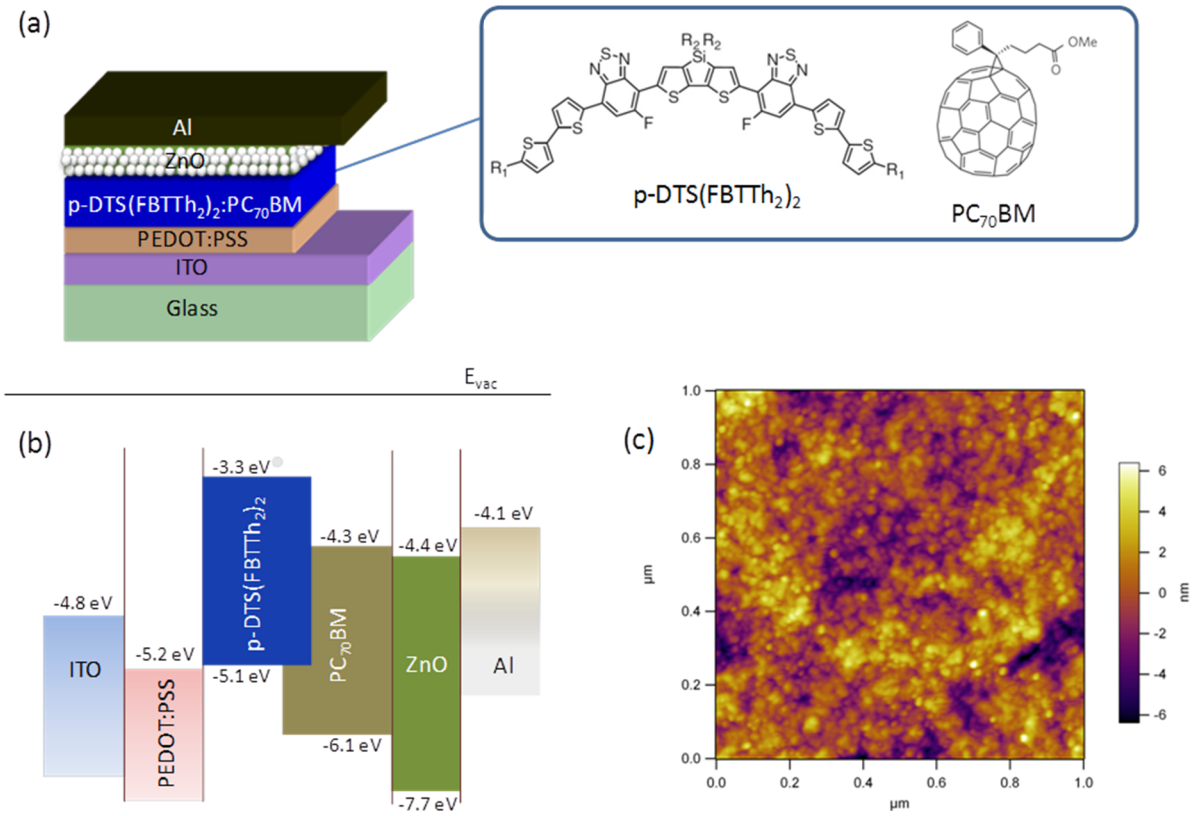

Figure 1. (a) Device structure of the solution-processed small molecule solar cell and molecular structure of p-DTS(FBTTh$_2$)$_2$ and PC$_{70}$BM. (b) Energy level diagram of the components of the solar cell. (c) AFM image of ZnO optical spacer.

While the exploitation of surface plasmon resonance effects may seem attractive, there are significant challenges for the incorporation of metal nanoparticles (NP) in the devices. The metal NP embedded in the active layer of OSC can enhance nonradiative decay processes and increase carrier recombination.[15] Although embedding the metal NP in the hole transport layer or coating the NP with insulating shell alleviates the aforementioned problems,[18−21] the induced electric field of the surface plasmon near a metal NP strongly decreases with radial distance from the NP and the light concentration factor is correspondingly reduced.[22,23]

On the other hand, it has been demonstrated that light absorption within thin layer can be enhanced by altering the spatial distribution of the optical electric field inside the cell.[24−27] Because of the optical interference between the incident and back-reflected light, the intensity of light at the surface of metal electrode is zero. Thus, the insertion of an optical spacer between the active layer and the metal electrode can place the active layer in a more favorable region of optical electric field. Herein, we demonstrate that this simple method is also effective for solution-processed SM solar cells and enhances the PCE of the cell without introducing any processing bottleneck and without any reduction in the electrical transport of the photogenerated carriers during sweep-out to the electrodes.

In our device design and optimization, we first tuned the thickness of the active layer to maximize the optical distribution inside the active layer and then inserted a layer of ZnO nanoparticles (cast from solution) as an optical spacer to further enhance the light absorption. We discovered that the ZnO optical spacer simultaneously improves the electrical properties of the solar cell while eliminating the need for vacuum-deposition and the need for using air-sensitive Ca as an interfacial layer. The combined electrical and optical improvements increase the PCE to 8.94% for the solution-processed SM solar cell using p-DTS(FBTTh$_2$)$_2$ and [6−6]-phenyl C$_{70}$ butyric acid methyl ester (PC$_{70}$BM) as the donor and the acceptor components, respectively. We also discuss the role of the ZnO nanoparticles (NP) in improving the optical and electrical properties by UV−vis absorption spectroscopy, the photoinduced carriers generation rate at saturated photocurrent, the charge collection probability, the hole blocking by the ZnO optical spacer, and reduction in the recombination loss.

Figure 1 shows the molecular structure of p-DTS(FBTTh$_2$)$_2$ and PC$_{70}$BM, the device structure, the energy levels of the components used in the devices, and an atomic force microscopy (AFM) image of the ZnO optical spacer deposited on the active layer. The ZnO optical spacer was prepared based on the work of Weller et al. and Janssen et al. (see Supporting Information for details).[28,29] Prior to the insertion of ZnO optical spacer between the active layer and Al electrode, we first optimized the thickness of active layer without optical spacer. Because of the interference between the incident and back-reflected light and refraction at the interfaces of multilayer stack, it has been observed that the optical interference peak does not necessarily increase with the thicker active layer in polymer-based OSC.[26,30,31] We also observed a similar trend here. Figure 2a and Table 1 show the current density−voltage (J−V) characteristics and electrical parameters of the cells with various thicknesses of active layer. The short-circuit current density (J_{SC}) reaches the maximum value (13.4 mA/cm^2) at the active bulk heterojunction (BHJ) layer thickness of 100 nm. At 120 nm thickness, J_{SC} drops to 12.8 mA/cm^2. The values shown

dx.doi.org/10.1021/nl401758g | Nano Lett. XXXX, XXX, XXX−XXX

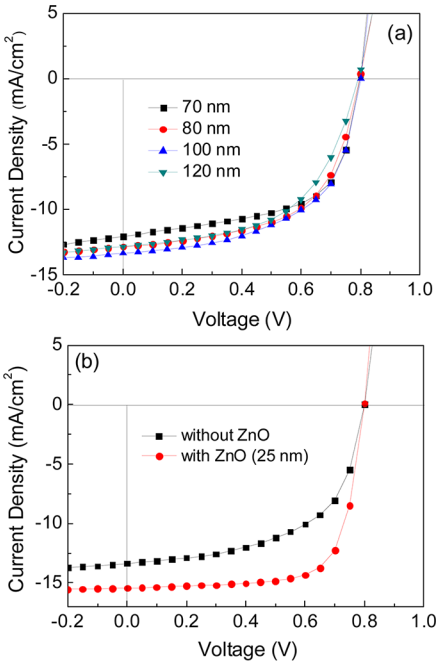

Figure 2. $J-V$ characteristics of p-DTS(FBTTh$_2$)$_2$:PC$_{70}$BM solar cells (a) with various thicknesses of active layer and (b) with and without optical spacer at the active layer thickness of 100 nm.

Table 1. Electrical Parameters of *p*-DTS(FBTTh$_2$)$_2$:PC$_{70}$BM Solar Cells with Various Thicknesses of Active Layer

thickness of active layer	J_{SC} (mA/cm^2)	V_{OC} (V)	FF (%)	PCE (%)
70 nm	12.1	0.797	60.6	5.83
80 nm	12.9	0.796	58.1	5.95
100 nm	13.4	0.795	56.5	6.02
120 nm	12.8	0.791	55.1	5.60

in Table 1 are based on the data obtained from the best device. The average values with their statistics from ten devices are shown in Supporting Information Table S1 and Figure S1.

After optimizing the thickness of the active layer, we insert the ZnO optical spacer (25 nm) between the active layer and Al electrode. The $J-V$ characteristics of the cells with and without optical spacers are shown in Figure 2b. The performance parameters are listed in Table 2. The J_{SC} and FF increase from

Table 2. Performance Parameters of *p*-DTS(FBTTh$_2$)$_2$:PC$_{70}$BM Solar Cells with and without ZnO Optical Spacer[a]

	J_{SC} (mA/cm^2)	V_{OC} (V)	FF (%)	PCE (%)
without ZnO	13.4	0.795	56.5	6.02
with ZnO	15.5	0.799	72.4	8.94

[a]The thickness of active layer is 100 nm.

13.4 mA/cm^2 and 56.5% to 15.5 mA/cm^2 and 72.4%, respectively. Hence, the PCE increases from 6.02% to 8.94%. Again, the values shown in Table 2 are based on the best device. The average values with their statistics from 10 devices are shown in Supporting Information, Table S2 and Figure S2. Despite no long-term stability data at this point, we observed that there is no serious degradation of device over a period of 8 days (Supporting Information, Figure S3).

To verify that the enhancement in J_{SC} is the result of the optical effect, we performed UV–vis absorption measurements and external quantum efficiency (EQE) measurements of the cells with and without ZnO NPs. The total absorption by the active layer (including the doubled path length in the active layer as a result of reflection from the Al electrode)[32] with and without ZnO NP were measured in reflection mode as shown in Figure 3a. Comparing two devices with the same active layer thickness (100 nm), an enhancement in absorption between 400 and 670 nm is observed in the cell with the optical spacer.

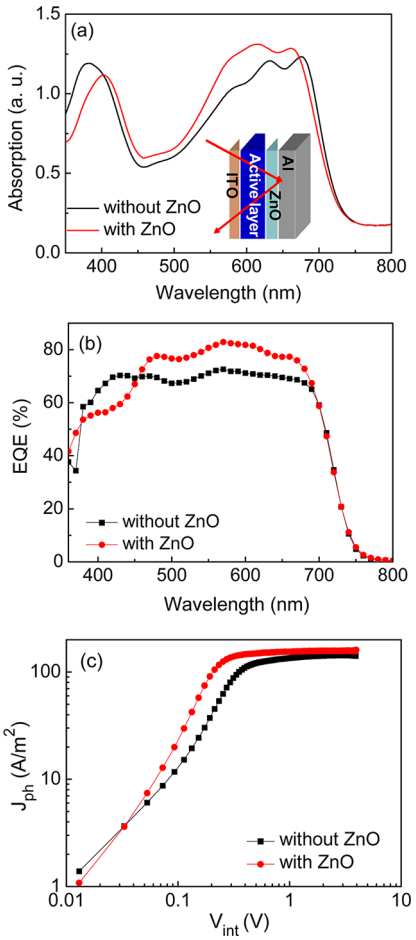

Figure 3. (a) Total absorption in the photoactive BHJ layer measured in a reflection geometry, (b) EQE spectra of the cells, and (c) photocurrent density as a function of internal voltage for the cells with and without a ZnO layer. The inset in Figure 4a shows a schematic of the device structure used for absorption measurements.

The enhanced absorption is in good agreement with the EQE spectra in which quantum efficiency increases between 450 and 700 nm (Figure 3b), to the value approaching 80%. There is a decrease in absorption and EQE at the short wavelength (around 400 nm) due to the insertion of ZnO. Nevertheless, the enhancement in absorption at longer wavelengths, especially near the absorption peak of the active layer, increases J_{SC}.

To further confirm the effect of ZnO on the optical properties of the solar cell, we experimentally determined the maximum photoinduced carriers generation rate (G_{max}) in devices with and without a ZnO layer. Figure 3c reveals the effect of the optical spacer on the photocurrent density (J_{ph})

dx.doi.org/10.1021/nl401758g | *Nano Lett.* XXXX, XXX, XXX–XXX

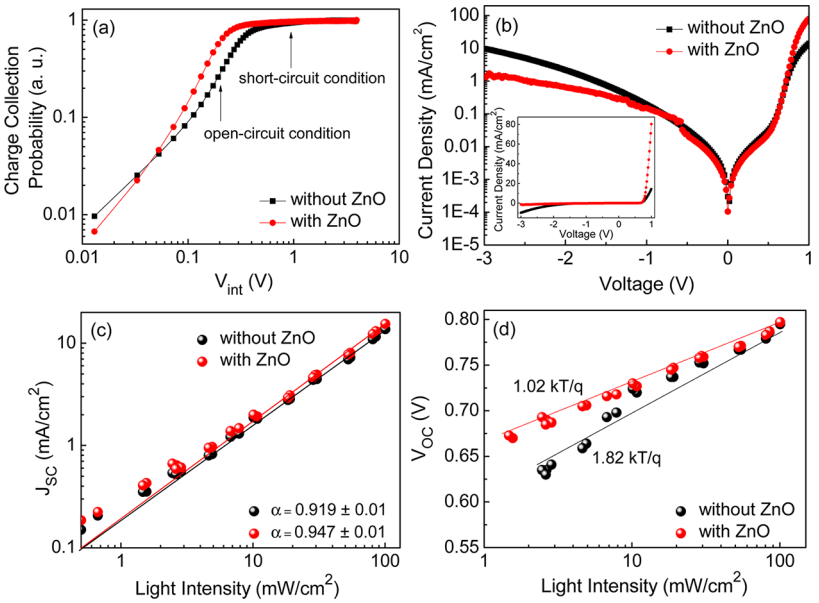

Figure 4. (a) Charge collection probability (or) normalized photocurrent with saturated photocurrent as a function of internal voltage for cells with and without ZnO layer. (b) $J-V$ characteristics of cells with and without ZnO layer swept from −3 V to +1 V in the dark. (c) Measured J_{SC} of cells with and without ZnO layer plotted against light intensity (symbols) on a logarithmic scale. Fitting a power law (solid lines) to these data yields α. (d) Measured V_{OC} of cells with and without ZnO layer as a function of light intensity (symbols), together with linear fits to the data (solid lines).

versus the internal voltage (V_{int}) of the device with and without ZnO layer, under illumination at 100 mW/cm^2. J_{ph} is calculated as $J_{ph} = J_L - J_D$, where J_L and J_D are the current density under illumination and in the dark, respectively.[33] V_{int} is determined as $V_{int} = V_{BI} - V_{app}$, where V_{BI} is the built-in voltage, which refers to the voltage at which J_{ph} is zero, and V_{app} is the applied voltage.[34]

Figure 3c shows that J_{ph} increases in proportion to the voltage at low V_{int}, but J_{ph} saturates at high V_{int} (2 V and above) where the internal field is large enough to sweep out all carriers to the electrodes. Therefore, the saturated photocurrent ($J_{ph,sat}$) is limited only by the number of absorbed photons. Thus,

$$J_{ph,sat} = qLG_{max} \quad (1)$$

where q is the elementary charge, L is the thickness of the active layer, and G_{max} is the maximum photoinduced carrier generation rate per unit volume.[35,36] The value of G_{max} for the cell without ZnO layer is 8.81×10^{27} m^{-3} s^{-1} ($J_{ph,sat}$ = 141.1 A/m^2), whereas that of G_{max} for the cell with ZnO layer increases to 1.00×10^{28} m^{-3} s^{-1} ($J_{ph,sat}$ =160.8 A/m^2). The data show a significant enhancement in G_{max} after inserting the ZnO optical spacer. As G_{max} corresponds to the maximum number of absorbed photons,[35,36] such enhancement implies that the absorption of light increases in the cell with the ZnO optical spacer.

As noted in the introduction, any technique employed for the enhancement in light absorption should not affect the carrier transport of the solar cell. To characterize the effect of ZnO layer on the electrical properties of the device, we examined the charge collection and blocking behavior in the cells with and without ZnO layer. Figure 4a shows the charge collection probability (P_C) with respect to V_{int} under illumination at 100 mW/cm^2. The J_{ph} of a solar cell can be written as,[33,37]

$$J_{ph} = qLG_{max}P_C \quad (2)$$

From the eqs 1 and 2, we can calculate P_C by normalizing J_{ph} with $J_{ph,sat}$ ($J_{ph}/J_{ph,sat}$).

As shown in Figure 4a, we see that P_C of the device with ZnO layer is higher than that of device without ZnO layer across the full range from short-circuit to open-circuit condition. The P_C increases from 90.5% to 96.2% at the short-circuit condition by inserting the ZnO layer. The increase in P_C is more significant at low V_{int} (high applied voltage). Thus, the ZnO optical spacer increases both the light absorption and charge collection, thereby enhancing J_{SC} by more than 15%. We observed that ZnO layer also effectively reduces the leakage current of diode at reverse bias. The $J-V$ characteristics of the cells with and without ZnO layer in the dark are shown in Figure 4b. There is serious leakage current at the negative bias in the device without ZnO, whereas a significant leakage current is not observed even at negative voltages as high as −3 V in the device with ZnO. The diode leakage current is reduced about 10-fold at −3 V by inserting the ZnO optical spacer. A high rectification factor of approximately 1000 (between −1 V and +1 V) is achieved in the device with ZnO.

To gain deeper insight into the influence of ZnO layer on the electrical properties of the cell, we studied the recombination mechanism with and without ZnO layer by measuring J_{SC} and open-circuit voltage (V_{OC}) at various light intensities from 100 to 0.9 mW/cm^2. A power law dependence of J_{SC} upon illumination intensity is generally observed in organic solar cells and can be expressed as

$$J_{SC} \propto I^{\alpha} \quad (3)$$

where I is the light intensity and α is the exponential factor.[33,35,38] The value α is close to unity, which is the result of weak bimolecular recombination during sweep-out.[38−40] In Figure 4c, the data are plotted on a log−log scale and fitted to a power law using eq 3: α = 0.947 and α = 0.919 for the cell with and without the ZnO layer, respectively, indicating that bimolecular recombination is reduced at short-circuit in the cell with the ZnO layer. This result agrees well with an increase in P_C from 90.5% to 96.2% at short-circuit and in FF from 56.5% to 72.4% by inserting the ZnO layer.

dx.doi.org/10.1021/nl401758g | Nano Lett. XXXX, XXX, XXX−XXX

The V_{OC} as a function of light intensity is shown in Figure 4d. The slope of V_{OC} versus the natural logarithm of the light intensity gives kT/q implying that bimolecular recombination is a dominant mechanism, where k, T, and q are the Boltzmann constant, temperature in Kelvin, and the elementary charge, respectively.[33,41] When the additional mechanism of Shockley–Read–Hall (SRH) or trap-assisted recombination is involved, a stronger dependence of V_{OC} on light intensity with a slope greater than kT/q is observed.[33,42] The slope of the cell with ZnO is $1.02kT/q$, whereas that of cell without ZnO is $1.82kT/q$, implying that ZnO reduces the density of interfacial traps between the BHJ and Al contact, and hence SRH recombination is suppressed.

In conclusion, we improved the absorption of light in solution-processed SM solar cells by optimizing the thickness of active layer followed by inserting a ZnO optical spacer between the active BHJ layer and the metal contact. The enhancement in light absorption in the cell was measured with UV–vis absorption spectroscopy and by measurements of the photo-induced carriers generation rate. The optical spacer improves the charge collection, improves the hole-blocking at the cathode, and simultaneously reduces the charge recombination. The combined electrical and optical improvements cause the PCE of solution-processed small-molecule solar cell to increase to 8.94%, that is, comparable to that of polymer counterparts.

■ ASSOCIATED CONTENT

Supporting Information

Detailed experimental section for the preparation of ZnO nanoparticles, fabrication of solar cells, characterization of devices and film, tables for average parameters of solar cells and their statistics, and initial stability test. This material is available free of charge via the Internet at http://pubs.acs.org.

■ AUTHOR INFORMATION

Corresponding Author

*E-mail: ajhe1@physics.ucsb.edu.

Author Contributions

A.K.K.K. and D.H.W. contributed equally to this work.

Notes

The authors declare no competing financial interest.

■ ACKNOWLEDGMENTS

Research at UCSB including the fabrication and testing of solar cells and the measurements and analysis were supported by the Institute for Collaborative Biotechnologies through grant W911NF-09-0001 from the U.S. Army Research Office. A.K.K.K. thanks Agency for Science Technology and Research (A*STAR) of Singapore for a postdoctoral fellowship. D. Wynands thanks DFG for funding by a research fellowship. Authors are grateful to support from the National Science Foundation under Grant No. NSF DMR-1121053, to the Materials Research Laboratory (MRL) and to the MRL staff.

■ REFERENCES

(1) Mishra, A.; Bäuerle, P. *Angew. Chem., Int. Ed.* **2012**, *51*, 2020–2067.
(2) Sun, Y.; Welch, G. C.; Leong, W. L.; Takacs, C. J.; Bazan, G. C.; Heeger, A. J. *Nat. Mater.* **2012**, *11*, 44–48.
(3) van der Poll, T. S.; Love, J. A.; Nguyen, T.-Q.; Bazan, G. C. *Adv. Mater.* **2012**, *24*, 3646–3649.
(4) Kyaw, A. K. K.; Wang, D. H.; Gupta, V.; Zhang, J.; Chand, S.; Bazan, G. C.; Heeger, A. J. *Adv. Mater.* **2013**, *25*, 2397–2402.
(5) Kyaw, A. K. K.; Wang, D. H.; Gupta, V.; Leong, W. L.; Ke, L.; Bazan, G. C.; Heeger, A. J. *ACS Nano* **2013**, *7*, 4569–4577.
(6) Walker, B.; Kim, C.; Nguyen, T.-Q. *Chem. Mater.* **2010**, *23*, 470–482.
(7) Wang, D. H.; Kyaw, A. K. K.; Gupta, V.; Bazan, G. C.; Heeger, A. J. *Adv. Energy Mater.* **2013**, DOI: 10.1002/aenm.201300277.
(8) Atwater, H. A.; Polman, A. *Nat. Mater.* **2010**, *9*, 205–213.
(9) Dennler, G.; Scharber, M. C.; Brabec, C. J. *Adv. Mater.* **2009**, *21*, 1323–1338.
(10) Peet, J.; Heeger, A. J.; Bazan, G. C. *Acc. Chem. Res.* **2009**, *42*, 1700–1708.
(11) Green, M. A.; Pillai, S. *Nat. Photonics* **2012**, *6*, 130–132.
(12) Nalwa, K. S.; Park, J.-M.; Ho, K.-M.; Chaudhary, S. *Adv. Mater.* **2011**, *23*, 112–116.
(13) Hsiao, Y.-S.; Chien, F.-C.; Huang, J.-H.; Chen, C.-P.; Kuo, C.-W.; Chu, C.-W.; Chen, P. *J. Phys. Chem. C* **2011**, *115*, 11864–11870.
(14) Lee, J. H.; Kim, D. W.; Jang, H.; Choi, J. K.; Geng, J.; Jung, J. W.; Yoon, S. C.; Jung, H.-T. *Small* **2009**, *5*, 2139–2143.
(15) Kulkarni, A. P.; Noone, K. M.; Munechika, K.; Guyer, S. R.; Ginger, D. S. *Nano Lett.* **2010**, *10*, 1501–1505.
(16) Ko, D.-H.; Tumbleston, J. R.; Zhang, L.; Williams, S.; DeSimone, J. M.; Lopez, R.; Samulski, E. T. *Nano Lett.* **2009**, *9*, 2742–2746.
(17) Long, Y. *Appl. Phys. Lett.* **2009**, *95*, 193301.
(18) Wu, J.-L.; Chen, F.-C.; Hsiao, Y.-S.; Chien, F.-C.; Chen, P.; Kuo, C.-H.; Huang, M. H.; Hsu, C.-S. *ACS Nano* **2011**, *5*, 959–967.
(19) Lu, L.; Luo, Z.; Xu, T.; Yu, L. *Nano Lett.* **2012**, *13*, 59–64.
(20) Qi, J.; Dang, X.; Hammond, P. T.; Belcher, A. M. *ACS Nano* **2011**, *5*, 7108–7116.
(21) Brown, M. D.; Suteewong, T.; Kumar, R. S. S.; D'Innocenzo, V.; Petrozza, A.; Lee, M. M.; Wiesner, U.; Snaith, H. J. *Nano Lett.* **2010**, *11*, 438–445.
(22) Zhu, J.; Xue, M.; Shen, H.; Wu, Z.; Kim, S.; Ho, J.-J.; Hassani-Afshar, A.; Zeng, B.; Wang, K. L. *Appl. Phys. Lett.* **2011**, *98*, 151110.
(23) Spinelli, P.; Polman, A. *Opt. Express* **2012**, *20*, A641–A654.
(24) Pettersson, L. A. A.; Roman, L. S.; Inganas, O. *J. Appl. Phys.* **1999**, *86*, 487–496.
(25) Kim, J. Y.; Kim, S. H.; Lee, H.-H.; Lee, K.; Ma, W.; Gong, X.; Heeger, A. J. *Adv. Mater.* **2006**, *18*, 572–576.
(26) Gilot, J.; Barbu, I.; Wienk, M. M.; Janssen, R. A. J. *Appl. Phys. Lett.* **2007**, *91*, 113520–3.
(27) Roy, A.; Park, S. H.; Cowan, S.; Tong, M. H.; Cho, S.; Lee, K.; Heeger, A. J. *Appl. Phys. Lett.* **2009**, *95*, 013302.
(28) Pacholski, C.; Kornowski, A.; Weller, H. *Angew. Chem., Int. Ed.* **2002**, *41*, 1188–1191.
(29) Beek, W. J. E.; Wienk, M. M.; Kemerink, M.; Yang, X.; Janssen, R. A. J. *J. Phys. Chem. B* **2005**, *109*, 9505–9516.
(30) Zhang, C.; Tong, S. W.; Jiang, C.; Kang, E. T.; Chan, D. S. H.; Zhu, C. *Appl. Phys. Lett.* **2008**, *93*, 043307.
(31) He, Z.; Zhong, C.; Su, S.; Xu, M.; Wu, H.; Cao, Y. *Nat. Photonics* **2012**, *6*, 591–595.
(32) Park, S. H.; Roy, A.; Beaupre, S.; Cho, S.; Coates, N.; Moon, J. S.; Moses, D.; Leclerc, M.; Lee, K.; Heeger, A. J. *Nat. Photonics* **2009**, *3*, 297–302.
(33) Cowan, S. R.; Roy, A.; Heeger, A. J. *Phys. Rev. B* **2010**, *82*, 245207.
(34) Cowan, S. R.; Street, R. A.; Cho, S.; Heeger, A. J. *Phys. Rev. B* **2011**, *83*, 035205.
(35) Mihailetchi, V. D.; Xie, H. X.; de Boer, B.; Koster, L. J. A.; Blom, P. W. M. *Adv. Funct. Mater.* **2006**, *16*, 699–708.
(36) Mihailetchi, V. D.; Koster, L. J. A.; Hummelen, J. C.; Blom, P. W. M. *Phys. Rev. Lett.* **2004**, *93*, 216601.
(37) Street, R. A.; Cowan, S.; Heeger, A. J. *Phys. Rev. B* **2010**, *82*, 121301.
(38) Riedel, I.; Parisi, J.; Dyakonov, V.; Lutsen, L.; Vanderzande, D.; Hummelen, J. C. *Adv. Funct. Mater.* **2004**, *14*, 38–44.
(39) Schilinsky, P.; Waldauf, C.; Brabec, C. J. *Appl. Phys. Lett.* **2002**, *81*, 3885–3887.

(40) van Duren, J. K. J.; Yang, X.; Loos, J.; Bulle-Lieuwma, C. W. T.; Sieval, A. B.; Hummelen, J. C.; Janssen, R. A. J. *Adv. Funct. Mater.* **2004**, *14*, 425−434.
(41) Koster, L. J. A.; Mihailetchi, V. D.; Ramaker, R.; Blom, P. W. M. *Appl. Phys. Lett.* **2005**, *86*, 123509.
(42) Mandoc, M. M.; Veurman, W.; Koster, L. J. A.; de Boer, B.; Blom, P. W. M. *Adv. Funct. Mater.* **2007**, *17*, 2167−2173.